



Study of the passivation of defects in the perovskite cell: application to Sahelian climate conditions

Essodossomondom Anate^{a,*}, N'Detigma Kata^{a,b}, Hodo-Abalo Samah^a, A. Seidou Maiga^b

^aFaculté des Sciences et Techniques, Université de Kara, Kara, Togo

^bLaboratoire Electronique, Informatique, Télécommunication et Energies Renouvelables, Université Gaston Berger, Saint-Louis, Sénégal

Abstract

This article is devoted to the study of the performance of the photovoltaic cell based on perovskite (MAPbI₃) in real conditions of sub-Saharan Africa. A model of this cell has been made taking into account the integration of defects at the interfaces. After a study of the sensitivity of these defects, a passivation layer was introduced at the interface to improve the performance of the cell. The influence of temperature and irradiance on the performance of perovskite cells was studied on the one hand with defects at the interfaces and on the other hand with the integration of a passivation layer of defects. The results show a decrease of the performance ratio for the non-passivated cell due to the defects present at the interfaces of the said cell. The models developed under SCAPS-1D were validated by applying it to a real module found in the literature under the same conditions. The performance calculation shows a satisfactory qualitative and quantitative agreement. The results relative to the performance ratios obtained for the simulated models show that perovskite is on the right track for a potential future candidacy to the most suitable technologies for sub-Saharan Africa.

DOI:10.46481/jnspss.2023.1250

Keywords: Modeling, perovskite solar cells, interface defects, performance ratio.

Article History :

Received: 30 December 2022

Received in revised form: 23 March 2023

Accepted for publication: 30 March 2023

Published: 14 May 2023

© 2023 The Author(s). Published by the Nigerian Society of Physical Sciences under the terms of the Creative Commons Attribution 4.0 International license (<https://creativecommons.org/licenses/by/4.0>). Further distribution of this work must maintain attribution to the author(s) and the published article's title, journal citation, and DOI.

Communicated by: K. Sakthipandi

1. Introduction

Africa has an almost unlimited potential for solar energy, estimated at about 10 TW [1]. However, Africa is among the regions in the world with the lowest coverage of electrical energy. Photovoltaics being the ideal alternative, solar fields are covering more and more surfaces using first generation modules which are relatively expensive and which moreover see their yields decrease under the influence of the temperature. Studies have shown the production capacity of thin-film technol-

ogy compared to first generation technology for sub-Saharan climate conditions [2,3]. Thus, this study is situated in the context of predicting the photovoltaic production under real sub-Saharan conditions of third generation thin film modules based on perovskite. The challenge is to evaluate the influence of climatic factors, in particular temperature, on the photovoltaic performance of these solar photovoltaic modules.

The interest of this technology is its very high efficiency of 25.5% in 2020 [4–6]. In addition, perovskite is a low-cost material with exceptional structural and optoelectronic properties. Tolerant in volume defects [6–8], it is not so when it comes to defects at the interfaces which in addition to lowering the yield,

*Corresponding author tel. no: +22893089314

Email address: edso.anate@gmail.com (Essodossomondom Anate)

makes it less stable in the long term. Of neutral, acceptor or donor nature, once at the interfaces, they significantly degrade the performance of the cell [7]. The most effective technique to minimize the influence of defects is passivation which uses materials with specific properties. Organic compounds with the carbonyl group are widely used to passivate perovskite cells [9] by exploiting the coordinated bonds based on Lewis's acid-base chemistry [10–12].

Wang *et al.* showed the passivation ability of theophylline ($C_7H_8N_4O_2$) on perovskite cells [9]. In this work, we examine the performance precisely the performance ratio of perovskite cells under sub-Saharan African conditions by simulation. Three perovskite modules, one of which is real [13] and two others modeled under SCAPS, are simulated under the same conditions. The purpose of the study of the latter two is to evaluate the impact of defects when the modules are operated in real conditions at high temperatures.

2. Methodology

We first model the cell under the SCAPS-1D software version 3.3.1.0 following the FTO/ETL/perovskite/HTL/Au structure by integrating at the ETL/perovskite and perovskite/HTL interfaces the neutral, acceptor and donor defects of the order of $10^8 - 10^{11} \text{ cm}^{-2}$ following Street *et al.* [8,14]. These three types of defects come either from vacancies (V_x) such as V_{MA} , V_{Pb} , V_I , or interstitials (X_i) like MA_i , Pb_i , I_i , or substitutions (X_y) such as MA_{Pb} , Pb_{MA} , MA_I , Pb_I , I_{MA} , I_{Pb} of the constituents (x or $y = MA, Pb, I$) [7] of the perovskite or of foreign elements. They can carry different electric charges behaving as electron acceptor, donor or neutral. Then a passivation layer based on theophylline is introduced following the structure FTO/ETL/Theophylline/perovskite/HTL/Au. The cell with defects at interfaces and the one with passivation layer were used to model tow modules. The data (V_{oc} , I_{sc} and P_{max}) from these models in addition to those from the real module which is from literature [13] are used in the hybrid Levenberg-Marquardt-analytical extraction program proposed by Kata *et al.* to extract the parameters (I_{ph} , I_0 , n , R_s and R_{sh}) needed for the simulation under LTSpice [15]. Finally, the sub-Saharan temperature and sunshine conditions are entered into the LTSpice module through the translation relations [15]. As an output, a current-voltage characteristic under real conditions is obtained for each measurement. Table 1 provides the information on module modeling considerations with reference to the real module. Figure 1 shows the method for evaluating the performance ratio of the module.

Solar irradiance and temperature data are taken from a measurement site in Ouagadougou (Burkina Faso) due to the unavailability of that site in Kara (Togo) at the moment.

These data such as temperature and irradiance are measured at the same time as module I-V characteristic, module voltage and module current by using multimeters simultaneously whereas a pyranometer was used to measure the irradiance as describe by Kata *et al.* [15]. Two days are chosen to represent the dry season for one and the rainy season for the other. The

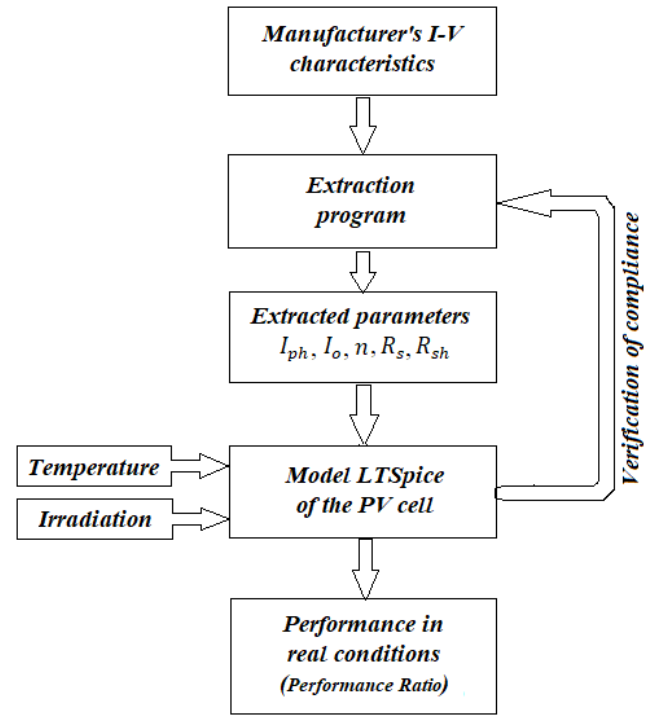


Figure 1: Diagram of the performance ratio evaluation

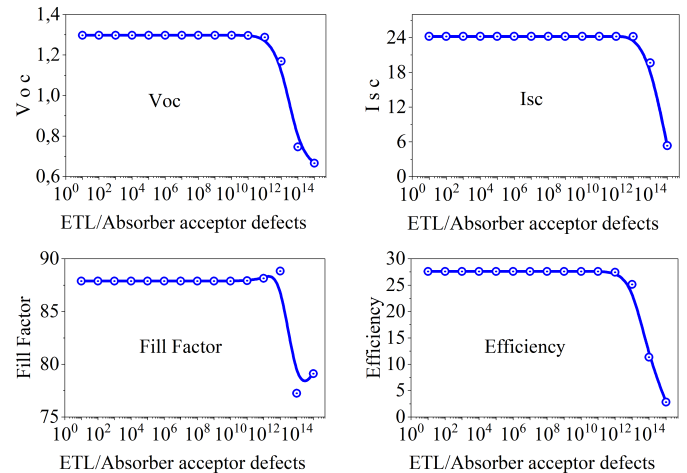


Figure 2: Effects of acceptor defects density at ETL/Absorber interface

performance evaluation is based on the calculation of the performance ratio (PR) of the three modules. The real efficiency (ϵ_{real}) of the LTSpice module is determined for each day's measurement using equation 1. The performance ratio allows comparison of this performance between the three modules under the same conditions. This ratio refers to the ratio of the real efficiency under real conditions (ϵ_{real}) to the efficiency under Standard Test Conditions (ϵ_{STC}) in equation 2. This Standard Test Conditions include the temperature of 25°C , AM1.5 and an irradiance of 1000 Wm^{-2} .

$$\epsilon_{real} = \frac{P_{mreal}}{S * G_{real}}, \quad (1)$$

Table 1: Characteristics of the simulated modules

PV module base on :	Passivated cell	Cell with defects	Real cell
Number of cells	55 in series	55 in series	55 in series
Efficiency (%)	27.87%	24.73%	17.9%
Voc (V)	71.61	63.86	58.7
Isc (A)	0.325	0.323	0.323
V _{max} (V)	64.9	58.3	48.42
I _{max} (A)	0.318	0.314	0.298
P _{max} (W)	20.6	18.25	14.43

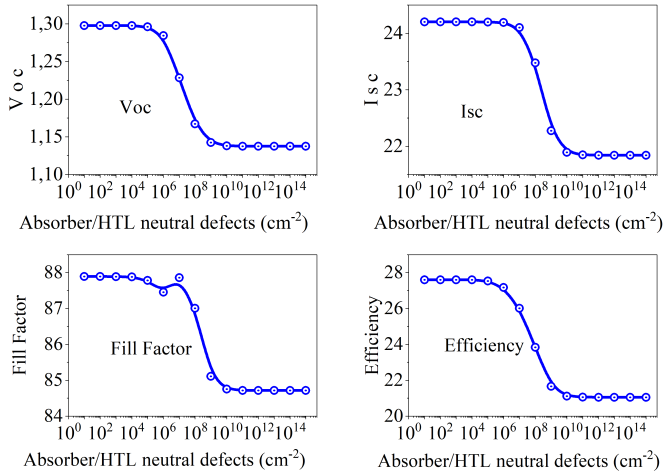


Figure 3: Effects of neutral defect density at Abs / HTL interface

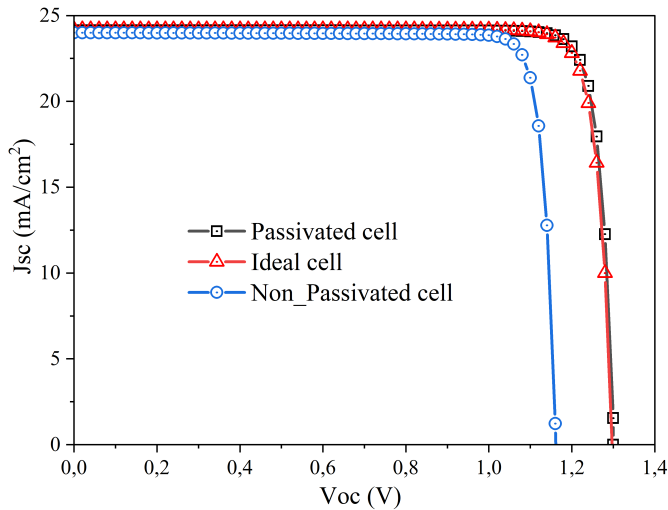


Figure 4: I-V characteristic of the simulated module

$$PR = \frac{P_{\text{real}}}{S G_{\text{real}}}, \quad (2)$$

where P_{real} is the maximum power under real conditions, S the surface of the module and G_{real} is the real condition solar irradiance.

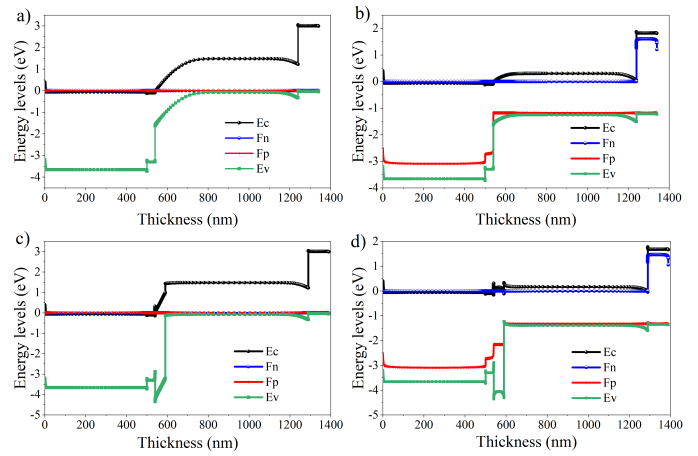


Figure 5: Energy band diagrams without (a, b) and with (c, d) passivation

3. Results and discussion

We studied the sensitivity of the defects at both interfaces varying from 1 to 10¹⁵ cm⁻². The drop in performance is felt from 10¹¹ cm⁻² at the ETL/perovskite interface for the three types of defects. Figure 2 illustrates this effect for the acceptor type with a drastic drop in Voc of 0.66 V, a Jsc of 4.53 mAcm⁻², a FF of 78.83% and a yield of 2.35% at 10¹⁵ cm⁻².

At the perovskite/HTL interface, the drop already starts at 10⁶ cm⁻² for all three types as well. At the perovskite/HTL interface (Figure 3), we note a decrease in Voc of 0.142 V and Jsc of 1.915 mAcm⁻² for neutral defect densities ranging from 10⁶ to 10⁹ cm⁻² which results in the loss of 2.34% of the FF and especially the yield which falls from 27.17% to 21.66% or a loss of 5.51%. This overall decrease can be explained by a low mobility of holes and therefore a low collection at the interface due to the introduction of larger neutral defects. Similar observations are made at other interfaces.

By applying the theophylline defect passivation layer whose electronic properties are derived from the work of Ejuh *et al.* [16], the results are presented in graphical form. Figure 4 shows the I-V characteristics of the ideal, passivated and non-passivated cells. A significant improvement in the Voc of the passivated cell compared to the non-passivated one is observed. This increase provides information about the recombination reduction.

We also observed the behavior of the band diagrams of the two modeled cells. The presence of defects (charged point de-

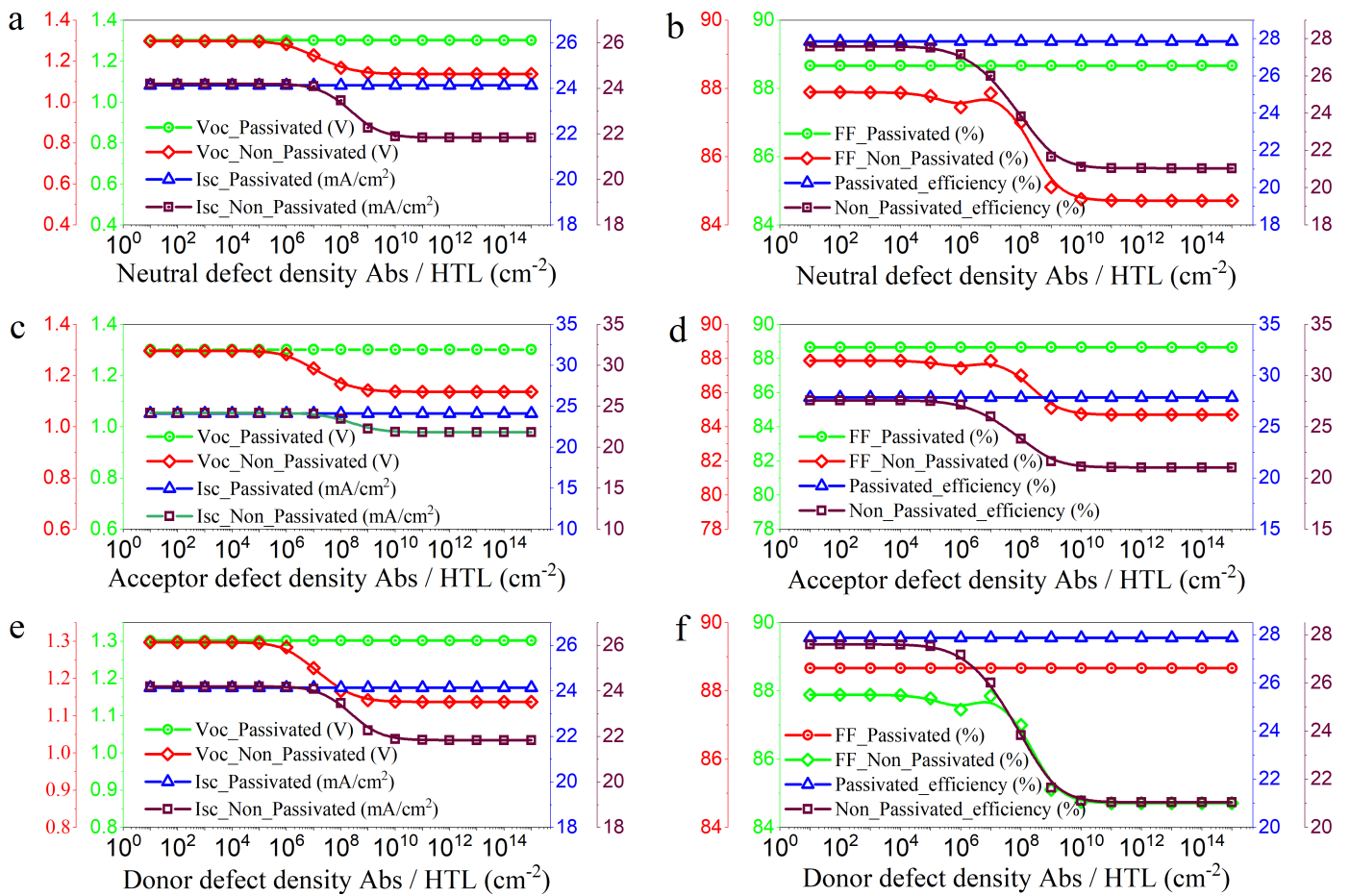


Figure 6: Comparison of the electrical characteristics of the cell without and with passivation

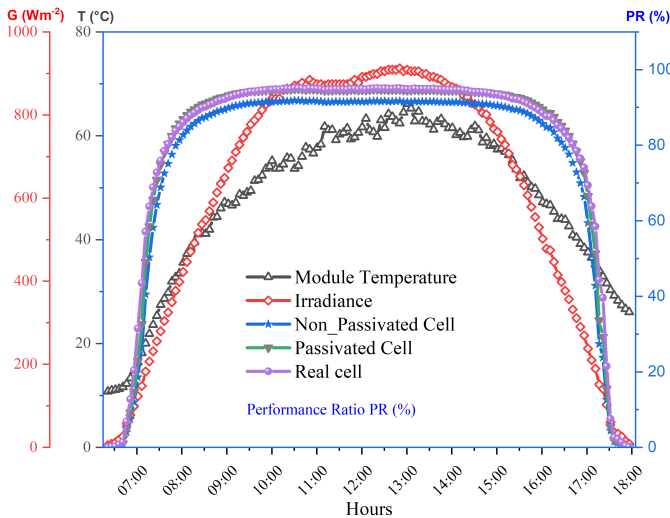


Figure 7: Performance ratio for a clear day (dry season)

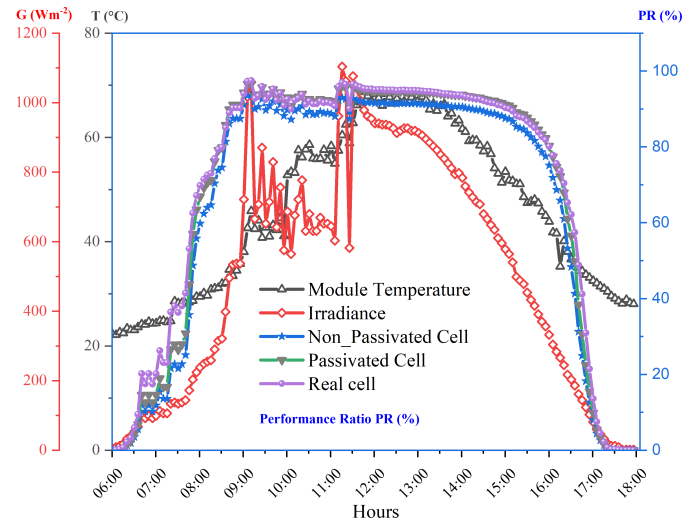


Figure 8: Performance ratio for an overcast day (Rainy season)

fects) at the interfaces manifests itself on the band diagram as unfavorable band edge curvature (possibly due to unintentional doping effect)[7,17]. Passivation reduced this unfavorable band curvature by eliminating the defects and their effect at the interface [17] to promote better performance such as improved open

circuit voltage by widening the potential barrier at the junction. Figures 5.a and 5.b show the band diagrams at equilibrium and at Voc for a cell with defects, respectively, followed by Figures 5.c and 5.d at equilibrium and at Voc for a passivated cell, respectively.

Here we present the performance of the modeled cells before and after passivation. The effect of the three types of defects at the perovskite / HTL interface is shown by a decrease in the graphs of Figure 6 from 10^6 cm^{-2} . The effect of passivation on the other hand is illustrated by straight lines giving as information the annihilation of the effect of these defects.

We present here on Figures 7 and 8 the production capacity in prediction of the performance under real conditions in Sub-Saharan Africa. The choice of two days for our study reflects the rainy season for the overcast day and the dry season for the clear day. The performance ratio of the three modules reaches 80% over most of the day for both days (Figures 7 and 8). For the clear-sky day, this ratio exceeds 90% between 9 a.m. and 3 p.m., a period during which there is often high irradiation. The strong dependence of the power of the module on the irradiation means that one could recover 90% of the power $P_{\text{max},STC}$ on more than half of the day, this one could even reach 94% and 96% respectively for the modules with not passivated and passivated cells then 98% for the real module. During the same period, high module temperatures exceeding 47°C are recorded.

However, the highest PRs are obtained during this period, moreover, there is no decrease in the ratio for the highest module temperatures of the day which are about 68°C . This means that the perovskite solar modules show only a small decrease in efficiency with high temperature. The real module and the module with passivated cells have very close ratios for both day conditions. However, the non-passivated cell shows much lower ratios over all the measurements. This low ratio is explained by the presence of defects at the interfaces of the cells of this module.

The evolution of the performance ratios of the real and passivated modules shows the relevance of the simulated models. Moreover, by observing the ratios of the two days we can say that the program responds well to the variations of the solar irradiation. Referring to Figure 8, it can be seen that perovskite modules have good ratios for overcast skies, which is an asset for some regions of sub-Saharan Africa that have longer rainy seasons with irregular irradiation. This interesting performance of perovskite allows us to consider perovskite as a potential future candidate of the most suitable technologies for the sub-region.

4. Conclusion

This study was devoted to the evaluation of the performance of perovskite cells under the conditions of sub-Saharan Africa. Different defects at the interfaces, namely neutral, acceptor and donor types, have been studied on the perovskite cell modeled under SCAPS-1D. The simulation of the model showed a strong sensitivity of the defects at the ETL/perovskite and perovskite/HTL interfaces of the cell. The results also show the performance improvement by introducing a passivation layer. The simulation of the perovskite solar cell in real conditions of sub-Saharan Africa is done. The hybrid Levenberg-Marquardt-analytic parameter extraction method proposed by Kata *et al.*

was used to extract the modeling data under LTSpice. The performance ratio of perovskite cells can reach 98% at module temperatures around 68°C in sub-Saharan African conditions. These results are quite interesting and encouraging for a possible use in the subregion.

References

- [1] BAD, "Énergies renouvelables: Pourquoi l'Afrique est la future grande puissance mondiale | Banque africaine de développement - Bâtir aujourd'hui, une meilleure Afrique demain," Nov. 22, 2021. [Online]. Available: <https://www.afdb.org/fr/news-and-events/why-africa-is-the-next-renewables-powerhouse-18822>. [Accessed: Nov. 22, 2021].
- [2] E. Anate, H.-A. Samah, and A. S. Maiga, "Simulation study of perovskite cell performance in real conditions of sub-Saharan Africa", TH Wildau Engineering and Natural Sciences Proceedings, **1** (2021). <https://doi.org/10.52825/thwildauensp.v1i.3>
- [3] N. Kata, D. Diouf, A. Darga, and A. S. Maiga, "The effect of the recombination mechanisms location on the temperature sensitivity of thin-film photovoltaic cells", EPJ Photovoltaics **10** (2019) 8.
- [4] M. Jeong, I. W. Choi, E. M. Go, Y. Cho, M. Kim, B. Lee, S. Jeong, Y. Jo, H. W. Choi, J. Lee, J.-H. Bae, S. K. Kwak, D. S. Kim, and C. Yang, "Stable perovskite solar cells with efficiency exceeding 24.8% and 0.3-V voltage loss", Science **369** (2020) 1615.
- [5] M. A. Green, E. D. Dunlop, J. Hohl-Ebinger, M. Yoshita, N. Kopidakis & X. Hao, "Solar cell efficiency tables (version 59)", Progress in Photovoltaics: Research and Applications **30** (2022) 3.
- [6] S. O. Bolarinwa, E. Danladi, A. Ichoja, M. Y. Onimisia & C. U. Achem, "Synergistic Study of Reduced Graphene Oxide as Interfacial Buffer Layer in HTL-free Perovskite Solar Cells with Carbon Electrode", Journal of the Nigerian Society of Physical Sciences **4** (2022) 909.
- [7] W.-J. Yin, T. Shi & Y. Yan, "Unusual defect physics in $\text{CH}_3\text{NH}_3\text{PbI}_3$ perovskite solar cell absorber", Applied Physics Letters **104** (2014) 063903.
- [8] D. Eli, M. Y. Onimisi, S. Garba, R. U. Ugbe, J. A. Owolabi, O. O. Ige, G. J. Ibeh & A. O. Muhammed, "Simulation and optimization of lead-based perovskite solar cells with cuprous oxide as a P-type inorganic layer", Journal of the Nigerian Society of Physical Sciences **1** (2019) 72.
- [9] R. Wang, J. Xue, K.-L. Wang, Z.-K. Wang, Y. Luo, D. Fenning, G. Xu, S. Nuryyeva, T. Huang & Y. Zhao, "Constructive molecular configurations for surface-defect passivation of perovskite photovoltaics", Science **366** (2019) 1509.
- [10] S. Sonmezoglu & S. Akin, "Suppression of the interface-dependent non-radiative recombination by using 2-methylbenzimidazole as interlayer for highly efficient and stable perovskite solar cells", Nano Energy **76** (2020) 105127.
- [11] D. Yang, X. Zhang, K. Wang, C. Wu, R. Yang, Y. Hou, Y. Jiang, S. Liu & S. Priya, "Stable efficiency exceeding 20.6% for inverted perovskite solar cells through polymer-optimized PCBM electron-transport layers", Nano letters, **19** (2019) 3313.
- [12] K. Liu, Q. Liang, M. Qin, D. Shen, H. Yin, Z. Ren, Y. Zhang, H. Zhang, P. W. Fong & Z. Wu, "Zwitterionic-surfactant-assisted room-temperature coating of efficient perovskite solar cells", Joule **4** (2020) 2404.
- [13] H. Higuichi & T. Negami, "Largest highly efficient $203 \times 203 \text{ mm}^2$ $\text{CH}_3\text{NH}_3\text{PbI}_3$ perovskite solar modules", Japanese Journal of Applied Physics **57** (2018) 08RE11.
- [14] R. A. Street, M. Schoendorf, A. Roy & J. H. Lee, "Interface state recombination in organic solar cells", Physical Review B **81** (2010) 205307.
- [15] D. Diouf, Y. M. Soro, A. Darga & A. S. Maiga, "Module parameter extraction and simulation with LTSpice software model in sub-Saharan outdoor conditions", African Journal of Environmental Science and Technology, **12** (2018) 523.
- [16] G. W. Ejuh, J. M. B. Ndjaka, F. T. Nya, P. L. Ndikum, C. Fonkem, Y. T. Assatse & R. Y. Kamsi, "Determination of the structural, electronic, optoelectronic and thermodynamic properties of the methylxanthine molecules theophylline and theobromine", Optical and Quantum Electronics **52** (2020) 1.
- [17] B. Chen, P. N. Rudd, S. Yang, Y. Yuan & J. Huang, "Imperfections and their passivation in halide perovskite solar cells", Chemical Society Reviews **48** (2019) 3842.